

Vertical Structure of Neutrino-Dominated Accretion Disk and Applications to Gamma-Ray Bursts

Tong Liu¹, Wei-Min Gu², Zi-Gao Dai¹, and Ju-Fu Lu²

ABSTRACT

We revisit the vertical structure of neutrino-dominated accretion flows in spherical coordinates. We stress that the flow should be geometrically thick when advection becomes dominant. In our calculation, the luminosity of neutrino annihilation is enhanced by one or two orders of magnitude. The empty funnel along the rotation axis can naturally explain the neutrino annihilable ejection.

Subject headings: accretion, accretion disks - black hole physics - gamma rays: bursts

1. Introduction

Gamma-Ray Bursts (GRBs) are short-lived bursts of gamma-ray photons occurring at cosmological distances. GRBs are usually sorted of two classes (Kouveliotou et al. 1993): short-hard GRBs ($T_{90} < 2\text{s}$) and long-soft GRBs ($T_{90} > 2\text{s}$). The likely progenitors are the merger of two neutron stars or a neutron star and a black hole (Eichler et al. 1989; Paczyński 1991; Narayan et al. 1992) and collapsar (Woosley 1993; Paczyński 1998), respectively. The popular model of the central engine, namely neutrino dominated accretion flows (NDAFs), involves a hyperaccreting black hole with mass accretion rates in the range of $0.01 \sim 10M_{\odot}\text{s}^{-1}$. Such a model has been widely investigated in the past decade (see, e.g., Popham et al. 1999; Narayan et al. 2001; Kohri & Mineshige 2002; Di Matteo et al. 2002; Rosswog et al. 2003; Kohri et al. 2005; Lee et al. 2005; Gu et al. 2006; Chen & Beloborodov 2007; Liu et al. 2007; Kawanaka & Mineshige 2007; Janiuk et al. 2007; Liu et al. 2008). The model can provide a good understanding of both the energetics of GRBs and the processes of making the relativistic and baryon-poor fireballs by neutrino annihilation or

¹Department of Astronomy, Nanjing University, Nanjing, Jiangsu 210093, China; tongliu@nju.edu.cn

²Department of Physics and Institute of Theoretical Physics and Astrophysics, Xiamen University, Xiamen, Fujian 361005, China; guwm@xmu.edu.cn

magnetohydrodynamic processes (see, e.g., Popham et al. [1999] and Di Matteo et al. [2002] for references).

In cylindrical coordinates (R, z, φ) , Gu & Lu (2007) discussed the potential importance of taking the explicit form of the gravitational potential for calculating slim disk (Abramowicz et al. 1988) solutions, and pointed out that the Hōshi form of the potential (Hōshi 1977),

$$\psi(r, z) \simeq \psi(r, 0) + \frac{1}{2}\Omega_K^2 z^2, \quad (1)$$

is valid only for geometrically thin disks with $H/R \lesssim 0.2$. Thus the well-known relationship $c_s/\Omega_K H = \text{constant}$ does not hold for slim disks with $H/R \lesssim 1$, where c_s is the sound speed, and Ω_K is the Keplerian angular velocity. Moreover, with the explicit form of the gravitational potential, Liu et al. (2008) found that NDAFs have both a maximal and a minimal possible mass accretion rate at their each radius, and presented a unified description of all the three known classes of optically thick accretion disks around black holes, namely Shakura-Sunyaev disks (Shakura & Sunyaev 1973), slim disks, and NDAFs. These works are, however, based on the following simple vertical hydrostatic equilibrium:

$$\frac{1}{\rho} \frac{\partial p}{\partial z} + \frac{\partial \psi}{\partial z} = 0, \quad (2)$$

instead of the general form (Abramowicz et al. 1997):

$$\frac{1}{\rho} \frac{\partial p}{\partial z} + \frac{\partial \psi}{\partial z} + v_R \frac{\partial v_z}{\partial R} + v_z \frac{\partial v_z}{\partial z} = 0, \quad (3)$$

where ρ is the mass density, p is the pressure, v_R is the cylindrical radial velocity, and v_z is the vertical velocity. Since v_z is not negligible for geometrically thick or slim disks, the solutions in Gu & Lu (2007) and Liu et al. (2008) are still not self-consistent. Recently, Gu et al. (2009) revisited the vertical structure in spherical coordinates and showed that advection-dominated accretion disks should be geometrically thick rather than being slim. However, the detailed radiative cooling was not considered in that work, and therefore no thermal equilibrium solution was established.

The purpose of this paper is to investigate the vertical structure of NDAFs with detailed neutrino radiation. In section 2, with the self-similar assumption in the radial direction, we numerically solve the differential equations of NDAFs in the vertical direction. In section 3, we present the vertical distribution of physical quantities and show the geometrical thickness and the energy advection of the disk. In section 4, we estimate the luminosity of neutrino annihilation and discuss some applications to GRBs. Conclusions are made in section 5.

2. Equation

We consider a steady state axisymmetric accretion flow in spherical coordinates (r, θ, ϕ) , i.e., $\partial/\partial t = \partial/\partial \phi = 0$. We adopt the Newtonian potential $\psi = -GM/r$ since it is convenient for self-similar assumption, where M is the mass of the central black hole. The basic equations of continuity and momentum are the following (see, e.g., Xue & Wang 2005; Gu et al. 2009):

$$\frac{1}{r^2} \frac{\partial}{\partial r} (r^2 \rho v_r) + \frac{1}{r^2 \sin \theta} \frac{\partial}{\partial \theta} (\sin \theta \rho v_\theta) = 0, \quad (4)$$

$$v_r \frac{\partial v_r}{\partial r} + \frac{v_\theta}{r} \left(\frac{\partial v_r}{\partial \theta} - v_\theta \right) - \frac{v_\phi^2}{r} = -\frac{GM}{r^2} - \frac{1}{\rho} \frac{\partial p}{\partial r}, \quad (5)$$

$$v_r \frac{\partial v_\theta}{\partial r} + \frac{v_\theta}{r} \left(\frac{\partial v_\theta}{\partial \theta} + v_r \right) - \frac{v_\phi^2}{r} \cot \theta = -\frac{1}{\rho r} \frac{\partial p}{\partial \theta}, \quad (6)$$

$$v_r \frac{\partial v_\phi}{\partial r} + \frac{v_\theta}{r} \frac{\partial v_\phi}{\partial \theta} + \frac{v_\phi}{r} (v_r + v_\theta \cot \theta) = \frac{1}{\rho r^3} \frac{\partial}{\partial r} (r^3 T_{r\phi}), \quad (7)$$

where v_r , v_θ , and v_ϕ are the three components of the velocity. Here, we only consider the $r\phi$ -component of the viscous stress tensor, $T_{r\phi} = \rho \nu r \partial(v_\phi/r)/\partial r$. The kinematic coefficient of viscosity takes the form: $\nu = \alpha c_s^2 / \Omega_K$ (e.g., Narayan & Yi 1995), where the sound speed c_s is defined as $c_s^2 = p/\rho$, the Keplerian angular velocity is $\Omega_K = (GM/r^3)^{1/2}$, and α is a constant viscosity parameter.

To avoid directly solve the above partial differential equations, some radial simplification is required since our main interest is the vertical distribution. Based on the radial self-similar assumption, Begelman & Meier (1982) studied the vertical structure of geometrically thick, optically thick, supercritical accretion disks. Under the same self-similar assumption, Narayan & Yi (1995) investigated the vertical structure of optically thin advection-dominated accretion flows (ADAFs). In fact, since the well-known self-similar solutions of ADAFs (Narayan & Yi 1994), such type of solutions has been widely investigated for different classes of accretion, such as slim disks (Wang & Zhou 1999), convection-dominated accretion flows (Narayan et al. 2000), NDAFs (Narayan et al. 2001), and accretion flows with ordered magnetic field and outflows (Bu et al. 2009). Even though the detailed radiation was considered in some works (e.g., Di Matteo et al. 2002; Chen & Beloborodov 2007), and

therefore the solutions cannot be regarded as self-similar solutions, the self-similar assumption was still adopted such that the original differential energy equation can be simplified as an algebraic one. Furthermore, for optically thick flows, Ohsuga et al. (2005) showed that their simulations are close to the self-similar solutions of the slim disk model (e.g., the density profile in their Fig. 11). In our opinion, the radial simplification is necessary for the study of vertical structure and it is a good choice to take the well-known self-similar assumption.

Similar to Narayan & Yi (1995), we adopt the following radial self-similar assumption:

$$\rho(r, \theta) \propto r^{-3/2}, \quad (8)$$

$$c_s(r, \theta), v_r(r, \theta), v_\phi(r, \theta) \propto r^{-1/2}, \quad (9)$$

$$v_\theta(r, \theta) = 0. \quad (10)$$

With the above assumption, equations (5-7) can be simplified as follows:

$$\frac{1}{2}v_r^2 + \frac{5}{2}c_s^2 + v_\phi^2 - r^2\Omega_K^2 = 0, \quad (11)$$

$$\frac{1}{\rho} \frac{dp}{d\theta} = v_\phi^2 \cot \theta, \quad (12)$$

$$v_r = -\frac{3}{2} \frac{\alpha c_s^2}{r \Omega_K}. \quad (13)$$

Integrating equation (4) over angle we obtain the mass accretion rate,

$$\dot{M} = -4\pi r^2 \int_{\theta_0}^{\frac{\pi}{2}} \rho v_r \sin \theta d\theta, \quad (14)$$

where θ_0 is the polar angle of the surface.

The equation of state is

$$p = p_{\text{gas}} + p_{\text{rad}} + p_e + p_\nu, \quad (15)$$

where p_{gas} , p_{rad} , p_e , and p_ν are the gas pressure from nucleons, the radiation pressure of photons, the degeneracy pressure of electrons, and the radiation pressure of neutrinos, respectively. Detailed expressions of the pressure components were given in Liu et al. (2007). We assume a polytropic relation in the vertical direction, $p = K\rho^{4/3}$, where K is a constant.

The energy equation is written as

$$Q_{\text{vis}} = Q_{\text{adv}} + Q_\nu, \quad (16)$$

where Q_{vis} , Q_{adv} , and Q_ν are the viscous heating rate per unit area, the advective cooling rate per unit area, and the cooling rate per unit area due to the neutrino radiation, respectively. Here we ignore the cooling of photodisintegration of α -particles and other heavier nuclei. The viscous heating rate per unit volume $q_{\text{vis}} = \nu\rho r^2[\partial(v_\phi/r)/\partial r]^2$ and the advective cooling rate per unit volume $q_{\text{adv}} = \rho v_r(\partial e/\partial r - p/\rho^2\partial\rho/\partial r)$ (e is the internal energy per unit volume) are expressed in the self-similar formalism as

$$q_{\text{vis}} = \frac{9}{4} \frac{\alpha p v_\phi^2}{r^2 \Omega_K}, \quad (17)$$

$$q_{\text{adv}} = -\frac{3}{2} \frac{(p - p_e)v_r}{r}. \quad (18)$$

where the entropy of degenerate particles is negligible. Thus the vertical integration of Q_{vis} and Q_{adv} are the following:

$$Q_{\text{vis}} = 2 \int_{\theta_0}^{\pi/2} q_{\text{vis}} r \sin \theta d\theta, \quad (19)$$

$$Q_{\text{adv}} = 2 \int_{\theta_0}^{\pi/2} q_{\text{adv}} r \sin \theta d\theta. \quad (20)$$

The cooling due to the neutrino radiation Q_ν can be written as

$$Q_\nu = 2 \int_{\theta_0}^{\pi/2} q_\nu r \sin \theta d\theta, \quad (21)$$

where q_ν is the sum of Urca processes, electron-positron pair annihilation, nucleon-nucleon bremsstrahlung, and Plasmon decay (see, e.g., Liu et al. 2007). We therefore can obtain the luminosity of neutrino radiation L_ν by integrating Q_ν .

In our system, we have six physical quantities varying with θ , i.e., v_r , v_ϕ , c_s , ρ , p , and T . The six equations for solving these quantities are equations (11-13), (15), the polytropic

relation, and the definition of c_s ($c_s^2 = p/\rho$). Three boundary conditions are required to solve the system since there is one differential equation, and the boundary θ_0 and the constant parameter K in the polytropic relation are unknown. Now we have already two boundary conditions, i.e., equations (14) and (16), thus one more boundary condition is required for solving the system, which is set to be $c_s = 0$ (accordingly $\rho = 0$ and $p = 0$, e.g., Kato et al. 2008, p. 244) at the surface of the disk, i.e., $\theta = \theta_0$. The numerical method is as follows. For given α , M , \dot{M} , r , and a test θ_0 , from the above six equations and two boundary conditions (except the energy equation, Eq. [16]), we can numerically obtain the vertical distribution of the above six quantities. With equations (19-21), we then check whether equation (16) is satisfied for the test θ_0 . By varying θ_0 we can find the exact value of θ_0 for which equation (16) is matched, and therefore we obtain the exact vertical distribution of all the variables. In our calculations we take $\alpha = 0.1$ and $M = 3M_\odot$.

3. Numerical Results

Figure 1 shows the variations of the density ρ , temperature T , electron fraction Y_e , and radial velocity v_r with the polar angle θ for $\dot{M} = 1M_\odot s^{-1}$. Here Y_e is defined as $Y_e \equiv n_p/(n_p + n_n)$, where n_p and n_n are the total number density of protons and of neutrons, respectively (e.g., Beloborodov 2003; Liu et al. 2007). The solid, dashed, and dotted lines represent the solutions at $r/r_g = 10, 40$, and 100 , respectively. The profiles of ρ and v_r are similar to that of the optically thin advection-dominated accretion flows (Narayan & Yi 1995), i.e., ρ and v_r (the absolute value) decrease from the equatorial plane to the surface. On the contrary, electron fraction Y_e increases from the equatorial plane to the surface and approaches 0.5 near the surface, which means that the matter is non-degenerate. The vertical distribution of v_r , as shown in Fig. 1(d), indicates a multilayer flow with the matter close to the equatorial plane being accreted much faster than that near the surface.

Figure 2(a) shows the variation of the half-opening angle of the disk ($\pi/2 - \theta_0$) with radius r/r_g , where $r_g = 2GM/c^2$ is the Schwarzschild radius. The solid, dashed, and dotted lines represent the solutions with $\dot{M}/M_\odot s^{-1} = 0.1, 1$, and 10 , respectively. It is seen that, in the inner region of the disk, the half-opening angle increases as increasing accretion rates. For $\dot{M} = 10M_\odot s^{-1}$, the inner disk is extremely thick with the half-opening angle is ~ 1.4 radian, which implies that there exists a narrow empty funnel $\sim 20^\circ$ along the rotation axis. Figure 2(b) shows the variation of the energy advection factor f_{adv} ($\equiv Q_{adv}/Q_{vis}$) with r/r_g . It is seen that advection becomes important in the inner disk for $\dot{M} \gtrsim 1M_\odot s^{-1}$. Comparing Figs. 2(a) and 2(b), we find that the curves of the half-opening angle and the advection factor are similar, which indicates that the geometrical thickness is relevant to

the advection. For $f_{\text{adv}} = 0.5$, it is seen from Fig. 2 that the half-opening angle is around 1.3 radian. We therefore stress that NDAFs should be significantly thick when advection becomes dominant, which is in agreement with Narayan & Yi (1995) since their solutions imply that the flows are extremely thick with the half-opening angle approaching $\pi/2$.

4. Applications to GRBs

In our calculations, the inner disk will be quite thick for large mass accretion rates, $\dot{M} \gtrsim 1M_{\odot}\text{s}^{-1}$. Thus the volume above the disk shrinks and the radiated neutrino density increases. Accordingly, the neutrino annihilation efficiency also increases. We have obtained the neutrino luminosity L_{ν} (before annihilation), thus the luminosity of neutrino annihilation $L_{\nu\bar{\nu}}$ can be roughly evaluated by the assumption: $\eta \propto V_{\text{ann}}^{-1}$ (see, e.g., Mochkovitch et al 1993), where $\eta \equiv L_{\nu\bar{\nu}}/L_{\nu}$ is the annihilation efficiency, and V_{ann} is the volume above the disk. For a given outer boundary r_{out} , we calculate V_{ann} by integrating the region of $\theta < \theta_0$ and $r < r_{\text{out}}$. The variations L_{ν} and $L_{\nu\bar{\nu}}$ with \dot{M} are shown in figure 3. The solid lines correspond to the present solutions whereas the dashed lines correspond to those in Liu et al. (2007). As shown in Fig. 3, for the same \dot{M} , L_{ν} is comparable, whereas $L_{\nu\bar{\nu}}$ in the present results is significantly larger than that in Liu et al. (2007) by one or two orders of magnitude. Moreover, we find that for $\dot{M} = 5M_{\odot}\text{s}^{-1}$, $L_{\nu\bar{\nu}}$ is very close to L_{ν} , which means that the density of radiated neutrino is so large that the annihilation efficiency is close to 1. Thus we can expect that $L_{\nu\bar{\nu}}$ is roughly equal to L_{ν} for $\dot{M} \gtrsim 5M_{\odot}\text{s}^{-1}$.

Many previous works have calculated the annihilation luminosity and claimed that the NDAF mode can provide enough energy for GRBs. However, GRBs are generally believed to be a jet with a small opening angle θ_{jet} . The problem is that, the annihilation could not be limited into such a small angle even though the region well above the inner disk have larger luminosity than other place. We argue that our model is preferably to explain the ejection-like radiation, because the disk is adequately thick and there exists a narrow empty funnel along the rotation axis, which can naturally explain the neutrino annihilable ejection.

5. Conclusions

In this paper we revisit the vertical structure of NDAFs in spherical coordinates. The major points we wish to stress are as follows:

1. We show the vertical structure of NDAFs and stress that the flow should be significantly thick when advection becomes dominant.

2. The luminosity of neutrino annihilation is enhanced by one or two orders of magnitude.
3. The narrow empty funnel ($\sim 20^\circ$) along the rotation axis can naturally explain the neutrino annihilable ejection.

We thank Katsuaki Asano, H.-Thomas Janka and Yi-Zhong Fan for beneficial discussion and comments. This work was supported by the National Basic Research Program (973 Program) of China under Grant 2009CB824800 (JFL and WMG), the National Natural Science Foundation of China under grants 10778711 (WMG), 10833002 (JFL and WMG), 10873009 (ZGD), and the China Postdoctoral Science Foundation funded project 20080441038 (TL).

REFERENCES

- Abramowicz, M. A., Czerny, B., Lasota, J.-P., & Szuszkiewicz, E. 1988, *ApJ*, 332, 646
- Abramowicz, M. A., Lanza, A., & Percival, M. J. 1997, *ApJ*, 479, 179
- Begelman, M. C., & Meier, D. L. 1982, *ApJ*, 253, 873
- Beloborodov, A. M. 2003, *ApJ*, 588, 931
- Bu, D.-F., Yuan, F., & Xie, F.-G. 2009, *MNRAS*, 392, 325
- Chen, W.-X., & Beloborodov, A. M. 2007, *ApJ*, 657, 383
- Di Matteo, T., Perna, R., & Narayan, R. 2002, *ApJ*, 579, 706
- Eichler D., Livio M., Piran T., & Schramm D. N. 1989, *Nature*, 340, 126
- Gu, W.-M., Liu, T., & Lu, J.-F. 2006, *ApJ*, 643, L87
- Gu, W.-M., & Lu, J.-F. 2007, *ApJ*, 660, 541
- Gu, W.-M., Xue, L., Liu, T., & Lu, J.-F. 2009, *PASJ*, in press (arXiv:0909.4838)
- Janiuk, A., Yuan, Y.-F., Perna, R., & Di Matteo, T. 2007, *ApJ*, 664, 1011
- Kato, S., Fukue, J., & Mineshige, S. 2008, *Black-Hole Accretion Disks: Towards a New Paradigm* (Kyoto: Kyoto Univ. Press)
- Kawanaka, N., & Mineshige, S. 2007, *ApJ*, 662, 1156
- Kohri, K., & Mineshige, S. 2002, *ApJ*, 577, 311
- Kohri, K., Narayan, R., & Piran, T. 2005, *ApJ*, 629, 341
- Kouvelietou, C., et al. 1993, *ApJ*, 413, L101
- Hōshi, R. 1977, *Prog. Theor. Phys.*, 58, 1191
- Lee, W. H., Ramirez-Ruiz, E., & Page, D. 2005, *ApJ*, 632, 421
- Liu, T., Gu, W.-M., Xue, L., & Lu J.-F. 2007, *ApJ*, 661, 1025
- Liu, T., Gu, W.-M., Xue, L., Weng, S.-S., & Lu J.-F. 2008, *ApJ*, 676, 545
- Mochkovitch, R., Hernanz, M., Isern, J., & Martin, X. 1993, *Nature*, 361, 236

- Narayan, R., Igumenshchev, I. V., & Abramowicz, M. A. 2000, *ApJ*, 539, 798
- Narayan, R., Paczyński, B., & Piran, T. 1992, *ApJ*, 395, L83
- Narayan, R., Piran, T., & Kumar, P. 2001, *ApJ*, 557, 949
- Narayan, R., & Yi, I. 1994, *ApJ*, 428, L13
- Narayan, R., & Yi, I. 1995, *ApJ*, 444, 231
- Ohsuga, K., Mori, M., Nakamoto, T., & Mineshige, S. 2005, *ApJ*, 628, 368
- Paczyński, B. 1991, *Acta Astronomica*, 41, 257
- Paczyński, B. 1998, *ApJ*, 494, L45
- Popham, R., Woosley, S. E., & Fryer, C. 1999, *ApJ*, 518, 356
- Rosswog, S., Ramirez-Ruiz, E., & Davies, M. B. 2003, *MNRAS*, 345, 1077
- Shakura, N. I., & Sunyaev, R. A. 1973, *A&A*, 24, 337
- Wang, J.-M., & Zhou, Y.-Y. 1999, *ApJ*, 516, 420
- Woosley, S. E. 1993, *ApJ*, 405, 273
- Xue, L., & Wang, J.-C. 2005, *ApJ*, 623, 372

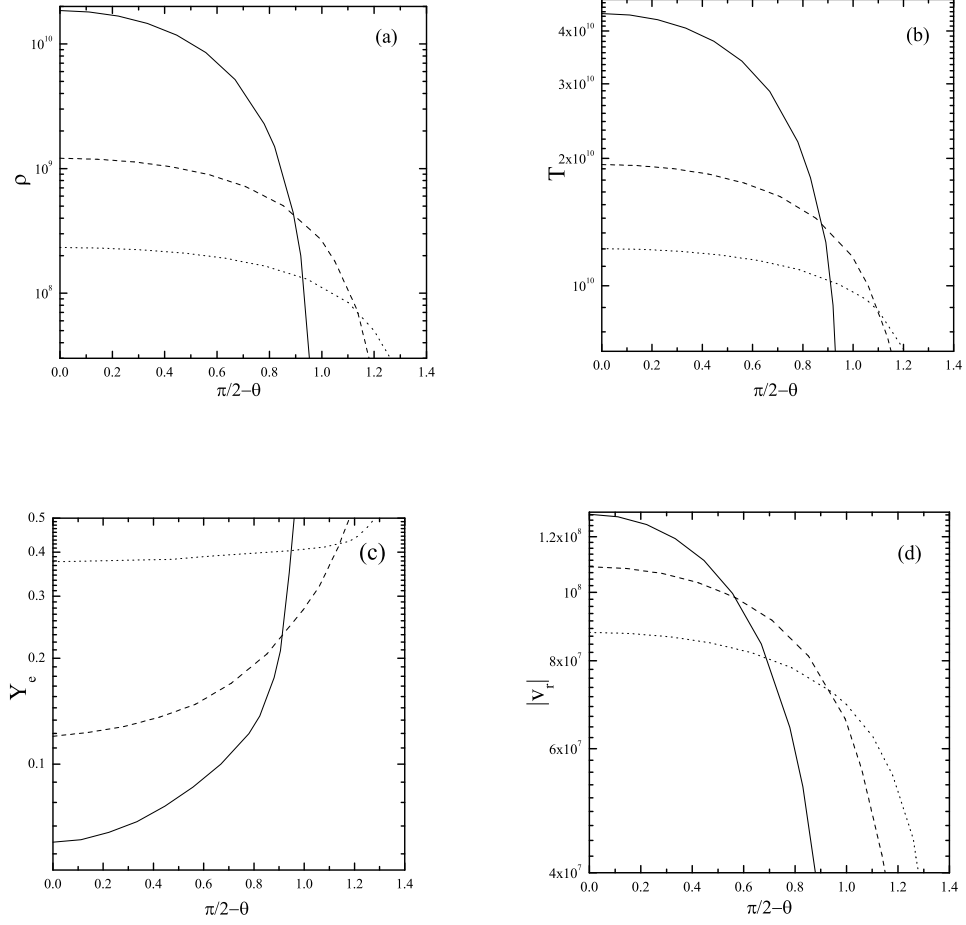


Fig. 1.— Variations of the density ρ , temperature T , electron fraction Y_e , and radial velocity v_r with the polar angle θ , for which the given parameters are $\dot{M}/M_\odot s^{-1} = 1$ and $r/r_g = 10$ (solid lines), 40 (dashed lines), 100 (dotted lines).

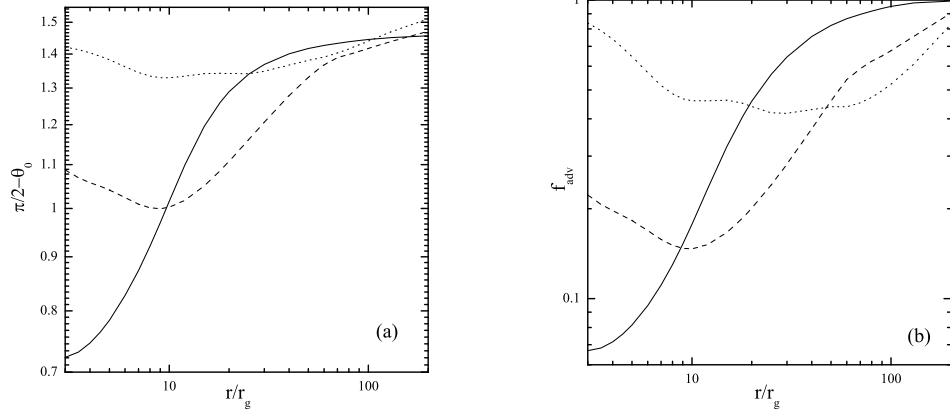


Fig. 2.— Variations of the half-opening angle of the disk ($\pi/2 - \theta_0$) and the advection factor f_{adv} with radius r/r_g , for which the given parameter is $\dot{M}/M_\odot \text{s}^{-1} = 0.1$ (solid line), 1 (dashed line), 10 (dotted line).

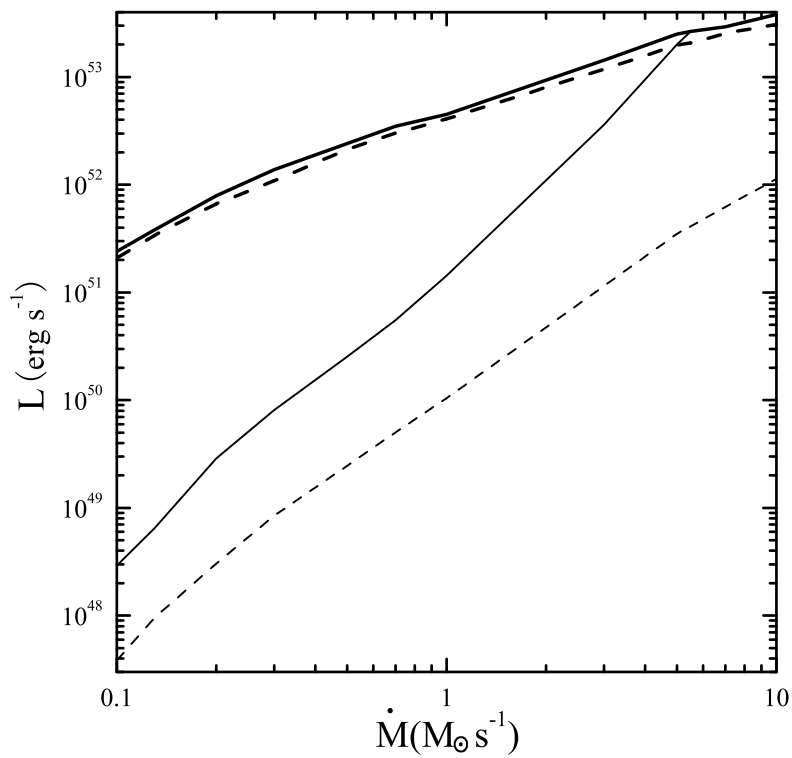


Fig. 3.— Neutrino luminosity L_{ν} (thick lines) and annihilation luminosity $L_{\nu\bar{\nu}}$ (thin lines) for varying mass accretion rates \dot{M} . The solid lines correspond to the present solutions, whereas the dashed lines correspond to the solutions of Liu et al. (2007).